Growth/differentiation factor 15 controls number of ependymal and neural stem cells in the ventricular/subventricular zone

Katja Baur[1], Carmen Carrillo-García[1], Şeydanur Şan[1,2], Manja von Hahn[1], Jens Strelau[3], Gabriele Hölzl-Wenig[1], Claudia Mandl[1], and Francesca Ciccolini[1]

[1]Department of Neurobiology, Interdisciplinary Center for Neurosciences (IZN), University of Heidelberg, Im Neuenheimer Feld 366, 69120 Heidelberg, Germany.
[2]Sorbonne University, 21 Rue de l'École de Médecine 75006 Paris, France.
[3]Department of Molecular Embryology, Institute of Anatomy & Cell Biology, University of Freiburg, Albertstr. 17, 79104 Freiburg, Germany.

Correspondence should be addressed to:
Dr Francesca Ciccolini
Email: ciccolini@nbio.uni-heidelberg.de
Phone: +49-6221-54 16505
Fax: +49-6221-54 16524

Key words: GDF15; GFRAL; EGFR; CXCR4; radial glia; subapical progenitors; neural stem cells; ganglionic eminence.

Acknowledgments: C.C. was supported by contract research from the program "Adult neural stem cell" of the Baden-Württemberg Stiftung. J.S. acknowledges the Deutsche Forschungsgemeinschaft (UN 34/23-1).

Abstract

Late in neural development, the expression of growth/differentiation factor (GDF) 15 increases in the germinal epithelium of the murine ganglionic eminence (GE). However, the function of GDF15 in this region is unknown. We here show that ablation of GDF15 leads to an increase in proliferation of apically and subapically dividing progenitors in the GE. This is associated with faster cell cycle progression in both progenitor groups, and an increase in the total number of cycling progenitors. Enhanced proliferation of apically dividing progenitors leads to a permanent significant increase in the number of ependymal and apical neural stem cells (NSCs). Our data also indicate that the extra proliferation of subapically dividing progenitors causes a transient increase in the number of neuronal progenitors, which is compensated by increased apoptosis. Independent of the genotype, activity of endogenous epidermal growth factor (EGFR) signalling is essential for the proliferation of apically and subapically dividing progenitors. However, lack of GDF15 leads to a reduced cell surface expression of EGFR and altered dynamics of MAPK activation in response to EGF stimulation. Application of exogenous GDF15 rescued the effect of the genotype on the expression of EGFR and decreased proliferation in the mutant GE. Taken together, our results indicate that GDF15 modulates proliferation and growth factor responsiveness of apical progenitors in the developing GE, thereby regulating the number of total ependymal and NSCs.

Introduction

Before the onset of neurogenesis, the wall of the neural tube is a pseudostratified epithelium named ventricular zone (VZ) (Huttner and Kosodo, 2005; McKay, 1997). Around the onset of neurogenesis, neuroepithelial cells in the VZ start to express several glial-associated genes and transform into radial glia (RG) (Hartfuss et al., 2001; Levitt and Rakic, 1980; Misson et al., 1988; Rakic, 1972). Both neuroepithelial cells and RG are apical progenitors connected to each other by adherens junctions at the apical cell surface and undergoing mitosis at the apical side of the VZ. All different types of neural cells derive directly or indirectly from RG through the generation of intermediate progenitors (Kosodo et al., 2004; Noctor et al., 2001; Noctor et al., 2008). Progenitors derived from RG include short neural progenitors (SNP) in the dorsal pallium (Tyler and Haydar, 2013), and subapical progenitors (SAP) first discovered in the subpallium (Pilz et al., 2013). Progenitors morphologically similar to SNPs were also observed in the developing subpallium, although it is unclear whether these apical progenitors with shorter basal processes represent SNPs or truncated RG, which wrap their basal process around blood vessels in the periventricular tissue (Tan et al., 2016). Both SNPs and SAPs display apical attachment, but whereas the first, like apical RG, undergo mitosis at the apical side of the VZ, the latter divide subapically. Apical RG also generate intermediate multipolar progenitors and elongated basal RG either directly or through the generation of SAPs (Petros et al., 2015; Pilz et al., 2013), which are collectively referred to as basal progenitors as they undergo cell division mostly at the basal side of the VZ, forming the secondary germinal epithelium termed subventricular zone (SVZ) (Haubensak et al., 2004; Kosodo and Huttner, 2009; Noctor et al., 2004). Whereas RG contribute to neurogenesis mostly indirectly by giving rise to more differentiated neuronal progenitors (Falk et al., 2017), SNPs and intermediate progenitors can undergo proliferative as well as differentiative cell divisions. The latter especially occur in cortical SNPs, which differ from their subpallium counterpart also because of slower cell cycle kinetics (Pilz et al., 2013; Stancik et al., 2010). In the ventral telencephalon, production of projection neurons (Matsushima and Graybiel, 2020) and interneurons (Kelly et al., 2018; Petros et al., 2015) continues until birth. During late mid-development RG give rise to ependymal cells (Spassky et al., 2008) and NSCs (Merkle et al., 2004), whereas at birth, most RG transform into astrocytes migrating to various brain areas (Culican et al., 1990; Voigt, 1989).

Aside from mode and site of division, VZ and SVZ progenitors differ with respect to several characteristics such as marker expression, duration of the cell cycle and cell coupling (Bittman et al., 1997; Calegari et al., 2005; Englund et al., 2005; LoTurco et al., 1991) to which contribute various regional-specific regulatory cues (Dause et al., 2022).

In this study, we have analysed the role of growth/differentiation factor (GDF)15, a member of the TGF-β superfamily, as a potential regulator of neural progenitor behaviour both in the embryonic and postnatal niche. In the adult brain, the choroid plexus epithelium of all ventricles represents the site of strongest and almost exclusive GDF15 expression in the adult CNS (Bottner et al., 1999; Schober et al., 2001). The neonatal brain displays GDF15 immunoreactivity not only in ependymal cells but also

in the SVZ (Schober et al., 2001), suggesting that it may affect progenitor cells. In line with this, GDF15 has also been implicated in proliferation and invasiveness of human glioblastoma (Gritti et al., 1999; Shnaper et al., 2009; Strelau et al., 2008). To investigate the potential role of GDF15 in the regulation of their behaviour, we have here analysed progenitors in the embryonic ganglionic eminence (GE) and in the postnatal SVZ of *Gdf15* deficient mice. Our observations provide first evidence that GDF15 regulates the proliferation rate of apically and subapically dividing progenitors in the embryonic and postnatal VZ, thereby controlling the total number of ependymal cells and NSCs in the adult V/SVZ.

Materials and Methods

Animals and tissue dissection

All animal experiments were approved by the Regierungspräsidium in Karlsruhe, Germany. Time-mated pregnant (plug day =1.0) and young adult (8 weeks) C57BL/6 wild type (WT) (Charles River) and *Gdf15* knock-out/lacZ knock-in ($Gdf15^{-/-}$) mice were killed by increasing CO_2 concentration followed by neck dislocation. The dissection of the embryonic GE was done to maximise the excision of the germinal region as described before (Ciccolini and Svendsen, 2001) in ice-cold Euromed-N basal medium (Euroclone). After dissection, the tissue was dissociated mechanically. Dissection and dissociation of the SVZ were done as described before (Cesetti et al., 2009).

$Gdf15^{+/-}$ matings were set up to obtain littermate embryos of the three genotypes (WT, $Gdf15^{-/-}$ homozygous and $Gdf15^{+/-}$ heterozygous). The generation of the $Gdf15^{-/-}$ line and the genotyping have been already described (Strelau et al., 2009).

BrdU labelling *in vivo*

Time-mated (E18) pregnant $Gdf15^{+/-}$ females from heterozygous matings were injected intraperitoneally with BrdU (10 μg/g body weight) once and sacrificed after 2 hours, or twice every two hours and killed 6 hours after the first injection.

Primary cultures

Neurosphere cultures were established and induced to differentiate as previously described (Gakhar-Koppole et al., 2008). During proliferation human recombinant EGF (20 ng/ml), FGF-2 (10 ng/ml) (Peprotech) and GDF15 (10 ng/ml) (R&D) were added to the culture medium as described. Differentiating cells were fixed and processed for immunostaining at different time points after plating as indicated in the text. In some experiments BrdU (6.7 μg/ml) was added to the media for 16 hours to label dividing cells. Thereafter cultures were processed for immunocytochemistry.

Clonal cultures were obtained by plating one cell per well, either by means of limiting dilutions or FACS automated deposition, in 96 well/plates in the presence of the above-mentioned concentration of EGF and FGF-2 with or without GDF15 as detailed in the text. For secondary sphere formation, primary clones were mechanically dissociated and replated at a density of 1000 cells per well in 96 well plates in EGF and FGF-2

supplemented culture medium. Confluence was measured using the IncuCyte S3 Live-Cell Analysis Instrument (Sartorius).

Fluorescence activated cell sorting (FACS)

Sorting was performed using a FACSVantage and a FACSAriaIII sorter (Becton Dickinson) as previously described (Carrillo-Garcia et al.; Cesetti et al., 2009; Ciccolini et al., 2005). For EGFR detection cells were stained in sort media with 20 ng/ml EGF conjugated to Alexa Fluor 488 or Alexa Fluor 647. For Prominin immunostaining cells were incubated one hour at 4°C with anti-Prominin-1 antibody conjugated to R-phycoerythrin (PE). Viable cells were revealed by propidium iodide (PI) exclusion (1 µg/ml, Sigma). All antibodies and labelled recombinant proteins used are listed in supplementary Table S1.

For β-galactosidase detection, dissociated cells obtained from Gdf15$^{+/-}$ animals were incubated in a solution containing Fluorescein Digalactopyranoside (FDG, Molecular Probes) and labelled according to the manufacturer's protocol.

Whole mounts preparation and treatment

For whole mount preparations, brain tissue of 8-weeks-old animals or E18 embryos was dissected as described before (Khatri et al., 2014), and the GE or SVZ was directly fixed in a 3% PFA / 4% sucrose solution in PBS for 24 h. Alternatively, the tissue was incubated in a well of a 24-well-plate containing 1 ml Euromed-N (Euroclone) with 1x B27 supplement (Invitrogen) and as indicated either a solvent control, human recombinant GDF15 (10 ng/ml; R&D Systems, 9279-GD), human recombinant EGF (20 ng/ml; Peprotech, #AF-100-15), PD158780 (20 µM; Calbiochem/Merck, #513035) or AMD3100 octahydrochloride hydrate (6 µM; Sigma Aldrich, # A5602) at 37°C, 5% CO_2 for 24h, and then fixed as described above.

For IdU labelling, E18 GEs were incubated in the same medium containing IdU (20 µM) for 1.5h and then either directly fixed as above, or incubated a further 12 h in Euromed-N with B27 without IdU, followed by fixation. The fixed tissue was kept in PBS containing 0.01% sodium azide at 4°C until immunostaining.

Western blot sample preparation

For western blot, the tissue of both GEs of one animal was mechanically dissociated in 600 µl Euromed-N with 1x B27 supplement, and the cell suspension was subsequently divided into 6 Eppendorf tubes á 100 µl. The cells were then treated with 100 µl additional medium containing, as indicated in the figure, either EGF (final concentration 20, 10, 5, 1 or 0.1 ng/ml) or GDF15 (final concentration 10 ng/ml) and incubated at 37°C, 5% CO_2 for 7 minutes in the Eppendorf tube or overnight (O/N) in a well of a 48-well plate to ensure air flow. Thereafter, the cell suspensions were either spun down at 2000 rpm and resuspended in 50 µl ice-cold RIPA buffer containing 1x protease inhibitor, or spun down at 1500 rpm and resuspended in fresh pre-warmed medium. Cell suspensions were then further incubated at 37°C for 30 min, 1h, 2h or 4h as indicated in the figure and afterwards harvested as above. Samples were kept at -20°C until western blot.

Samples were mixed with 4x Laemmli buffer and run on a standard 7.5% SDS-polyacrylamide gel at a constant current of 30 mA per gel for 80-90 min on ice, then transferred onto a nitrocellulose membrane (Whatman Protran BA85, pore size 0.45 µm, Sigma-Aldrich) at a constant voltage of 20 V for 2h at RT. The membrane was blocked in 5% milk in tris-buffered saline containing 1% Tween-20 (TBS-T), and incubated with primary antibodies in TBS-T O/N at 4°C on a shaker. After washing with TBS-T, secondary antibodies conjugated to horseradish peroxidase were applied in 5% milk in TBS-T for 1h at RT on a shaker. Signal was detected with Amersham ECL Western Blotting Detection Reagent (GE Healthcare) using a Chemidoc Imaging System (Bio-Rad Laboratories).
All antibodies used for Western Blot are listed in supplementary Table S2.

Immunofluorescence

For cell cultures

Cells were fixed with 3% paraformaldehyde (PFA) in PBS containing 4% sucrose for 10 min at RT and permeabilised with NP-40 (0.5%). For BrdU stainings, cells were incubated with HCl 2 N for 30 minutes followed by a wash with sodium tetraborate 0.1 M pH 8.5. After permeabilisation, cells were incubated with primary antibodies O/N at 4°C and then with fluorescently labelled secondary antibodies for 1 hour at room temperature. The detection of O4 was done by incubating primary antibodies on live cells at 37°C. Nuclei were counterstained with 4',6-Diamidine-2'-phenylindole-dihydrochloride (DAPI; Roche).

For brain slices

Adult mice were anesthetised with an intraperitoneal injection of sodium-pentobarbital (2 ml/kg body weight; Narcoren®, Merial, Germany) and perfused with 4% paraformaldehyde (PFA), whereas brains from E18 WT and *Gdf15*$^{+/-}$ littermates were fixed by immersion in 4% PFA O/N. Thereafter, the tissue was cryoprotected by transfer into 30% sucrose O/N and then embedded in Tissue-Tek and frozen. Coronal slices 16 µm thick were cut with a cryostat (Leica CM3050S). Slices were permeabilised with 0.5% NP-40. For BrdU staining, slices were sequentially exposed to the following solutions in PBS: HCl 2 N, sodium tetraborate 0.1 M pH 8,5, glycine 0.1 mM, ammonium chloride 50 mM, and finally 5% FCS for one hour. Incubation with primary and secondary antibodies with DAPI was performed O/N at 4ºC and for one hour at room temperature, respectively.

For whole mounts

Whole SVZ / GE tissue was fixed as indicated above, briefly rinsed in 10 mM glycine, and permeabilized with 0.5% NP-40 for 10 min. To reduce background and unspecific staining, the tissue was incubated in 100 mM glycine and blocked with 5% FCS, 0.1% NP-40 for 1.5h at room temperature. Primary antibodies were applied in 0.1% NP-40 at 4°C O/N, and secondary antibodies and DAPI were applied in 5% FCS, 0.1% NP-40 for 2h at RT after washing. The tissue was mounted on glass slides using mowiol.

If not otherwise indicated, all solutions were diluted in PBS and all steps performed at RT. All antibodies used for immunofluorescence are listed in supplementary Table S3.

Imaging of immunolabelled cells and slices

Fluorescent micrographs were acquired using an Axioplan 2 imaging microscope (Zeiss, Germany) equipped with a AxioCam digital camera (AxioCam HRc Zeiss, Germany) and AxioVision software (AxioVs40 V 4.5.0.00, Carl Zeiss Imaging, Germany). Confocal micrographs were acquired with a laser scanning confocal microscope (TCS SP2 scanning head and inverted DMIRBE microscope, 40x oil immersion HCX PL APO objective, Leica confocal scan (LCS) software; Leica, Germany).

Confocal imaging of whole mounts

At least 3 different fields of view any individual whole mount was imaged using a Leica TCS SP8 confocal microscope with a 40x or 63x oil immersion objective and LASX software (Leica). Images were acquired as z-stacks with 18-22 µm thickness with a z-step of 1 µm. The images displayed in the figures are complete or partial z-projections of the stack performed with Fiji/ImageJ (Schindelin et al., 2012).

Image analysis

Images were analysed using Fiji/ImageJ software (Schindelin et al., 2012); Ki67, IdU/BrdU and phH3 cells were counted manually using the "Cell Counter" plugin if they contained visible nuclear staining.

For each antigen at least three animals were analysed. For each mouse three sections at comparable rostrocaudal levels and separated from each other by five intervening sections (80 µm in total) were counted.

Real time PCR

RNA isolation was performed using the TriFast reagent (peqlab) or Quick-RNA Micro Prep Kit (Zymo Research) according to the manufacturer's protocol. RNA concentration was measured by optic densitometry using an Eppendorf BioPhotometer. Total RNA was retrotranscribed into cDNA using M-MLV reverse transcriptase with Oligo(dT)15 primers (Promega) according to manufacturer's instructions. qPCR for the genes of interest was performed using the TaqMan gene expression assays and the StepOnePlus System (Applied Biosystems). Gene-specific TaqMan probes for the genes of interest *Gdf15*, *Gfral*, *Fgf-2*, *Fgf* receptors 1 and 2, and housekeeping genes 18s, *Gapdh* and *β-Actin* were obtained from Applied Biosystems as Assays-on-Demand (AOD) gene expression products. The AOD ID's were *Gdf15* Mm00442228-m1; *Gfral* Mm02344882_m1; *Fgf-2* Mm00433287-m1; *Fgfr1* Mm00438923-m1; *Fgfr2* Mm00438941-m1; 18s, Hs99999901-s1; *Gapdh*, Mm00000015-s1; *β-Actin*, Mm00607939-s1. *Egfr* and *Gfral* transcripts as indicated were determined with PowerTrack SYBR Green (ThermoFisher) and the following primers: *Egfr* mouse forward 5'-ACCTCTCCCGGTCAGAGATG-3', *Egfr* mouse reverse 5'-CTTGTGCCTTGGCAGACTTTC-3' (Kefaloyianni et al., 2016); *Gfral* mouse forward 5'-GGGATGTTGGTTGGTGTCAG-3', *Gfral* mouse reverse 5'-

AGGCAGGTGTCTTCCATTGA-3'. Results were expressed as $2^{-\Delta\Delta CT}$ which is an index of the relative amount of mRNA present in each sample.

Results

GDF15 is expressed both in apical progenitors and intermediate precursors

Previous studies have reported very low levels of *Gdf15* mRNA and protein in neural tissues. The highest levels of GDF15 protein expression were observed within the germinal epithelium lining the lateral ventricle and in the choroid plexus in neonatal and adult rats, respectively (Bottner et al., 1999; Schober et al., 2001). Levels of *Gdf15* transcripts increase in the embryonic GE from late development onwards (Carrillo-Garcia et al., 2014). They remain high in the corresponding adult cortical tissue in the postnatal V/SVZ indicating that also in this germinal niche GDF15 may affect neurogenesis, as previously observed in the subgranular zone of the hippocampus (Carrillo-Garcia et al., 2014). Consistent with these previous observations, *Gdf15* transcripts were expressed in GE/SVZ neurosphere-derived progenitors (supplementary Fig. S1A) and GDF15 immunoreactivity was present in SOX2 and EGFR expressing progenitors in the adult V/SVZ (Fig 1A). We next investigated the expression of the GDNF Family Receptor Alpha-Like (GFRAL), which has recently been identified as the GDF15 receptor (Li et al., 2017; Mullican et al., 2017; Yang et al., 2017), by qPCR (supplementary Fig. S1B-D) and by immunostaining (Fig. 1B). Both analyses revealed expression of the receptor in the E18 GE, with immunostaining showing a particular presence of the protein around the ventricular area (Fig. 1B). A similar pattern of expression was also observed in the adult V-SVZ, albeit at a lower level than in the embryonic tissue (Fig. 1C). Taken together, our analyses show that GDF15 is particularly expressed in the germinal region of the GE and the adult V-SVZ, which largely derives from the former. They also show that GDF15 expressing cells include NSC like progenitors.

GDF15 affects the proliferation of apically and subapically dividing progenitors in the embryonic GE

Expression of both ligand and receptor in this region suggests a biological function of the growth factor in developing and adult progenitors. To begin to answer this question, we next used flow cytometry to quantify the number of apical P^+ progenitors in the WT and $Gdf15^{-/-}$ E18 GE, as this region displays high levels of expression of both receptor and growth factor. Compared to the WT control, more P^+ apical progenitors were present in the mutant tissue (Fig. 2A). The proliferation of progenitors was also increased in the mutant GE as shown by quantification of the number of Ki67 immunopositive cells in whole mount preparations (Fig. 2B, C). Besides the number of total cycling cells in the mutant VZ, the mutation also led to a strong increase in the number of mitotic progenitors, counted based on the morphological nuclear appearance to score mitotic figures in anaphase and telophase (Fig. 2B white arrow, D). This analysis allowed us to distinguish between apically dividing progenitors, i.e RG and SNPs, and SAPs undergoing mitosis at subapical locations of the VZ. We found that mitotic figures were increased in both groups of progenitors increased in the mutant tissue at E18 (Fig. 2D).

A similar change was also observed in the adult V/SVZ with more cells undergoing apical division in mutant 8-week-old (8W) animals than in age-matched counterparts (supplementary Fig. S2A, B). To better understand the effect of GDF15 ablation on proliferation, we incubated whole tissue explants in medium containing IdU for 1.5 hours and investigated cells undergoing DNA replication immediately thereafter or after further 12 hours of incubation in medium without IdU (Fig. 2E, F). At both time points, more IdU^+ progenitors were scored in the mutant tissue (Fig. 2F). At the earliest time point, extra IdU^+ progenitors included both mitotic apically dividing progenitors as well as SAPs, as determined by the expression of phospho-Histone H3 (phH3). However, the number of mitotic IdU^- cells was not affected and it showed a trend decrease compared to the WT control, indicating that absence of GDF15 leads to a shortening of the transition between the S and M phases of the cell cycle and possibly of the duration of the M phase. Supporting this hypothesis, the effect of the genotype on $phH3^+$ mitotic figures, which include all cells in M phase, was smaller than the effect on $Ki67^+$ mitotic figures (Fig. 2 compare panels D and F), which scores only cells in advanced stages of mitosis. Finally, whereas at the earlier time point the genotype did not affect IdU immunofluorescence levels (Fig. 1E, upper panels), 12 hours after IdU withdrawal more cells displaying light IdU immunoreactivity were present at the apical side of the mutant GE than in the WT counterpart, (Fig. 2E, lower panels). This indicates that after DNA replication and division, more apical cells remain at the apical side in the mutant GE than in the WT counterpart, which is consistent with the higher number of $Prominin^+$ cells in the mutant GE. Supporting this conclusion, at this time, the number of IdU^+ cells undergoing mitosis at the apical border was still increased in the mutant tissue, whereas mutant IdU^+ mitotic SAPs displayed only a trend increase that was not significant (Fig. 2F). To investigate whether the genotype affects cell cycle re-entry, we also analysed the percentage of cells which were still cycling after having replicated their DNA (supplementary Fig. S2C, D). After 1.5 hours in the presence of IdU, lack of GDF15 significantly altered the proportion of both cycling and non-cycling IdU^+ progenitors, the effect being significant only the first group (supplementary Fig. S2C). However, after 12 hours, all the extra IdU^+ cells in the mutant GE had exited the cell cycle (supplementary Fig. S2D), showing that the extra proliferating cells in the mutant GE do not represent a population of continuously cycling progenitors. We next investigated the cell division angles relative to an axis orthogonal to the ventricular surface, to see if apical extra proliferation is associated with an increase in symmetrically dividing cells (Fig. 3A-E). Both at E18 and 8W, most apically dividing cells divided with a 0° angle (i.e., symmetrically) in both genotypes (Fig. 3A, C). In the embryonic tissue, about 40% of dividing cells displayed a 45° angle (asymmetrically; Fig. 3D). This number decreased to less than 20% in the adult animals (Fig. 3E), indicating a decrease in neurogenic divisions while NSC maintaining divisions persist (Chenn and McConnell, 1995; Zhang et al., 2004). Thus, the $Gdf15^{-/-}$ V/SVZ has a higher number of cells undergoing mitosis but the distribution of division mode is not changed compared to the WT control at either age. This indicates that GDF15 affects the number of apically dividing cells without changing the orientation of the division plane. Finally, we investigated whether GDF15 directly affects proliferation by applying exogenous GDF15 in the medium. Treatment

of Gdf15$^{-/-}$ E18 GE whole mounts for 24 hours normalized the number of cycling progenitors to WT levels (Fig. 3F), and it reduced the number of mitotic SAPs and apically dividing progenitors in explants of the mutant GE (Fig. 3G). In contrast, the treatment largely did not alter the proliferation in the WT GE, with the exception of a significant increase in the number of apically dividing progenitors (Fig. 3G). Taken together, our data are consistent with a direct effect of GDF15 on progenitor proliferation in the embryonic GE. They also highlight that although GDF15 affects cell division in both the WT and mutant GE, the effect of the growth factor is different in WT and mutant progenitors.

Lack of GDF15 affects EGFR expression and EGF responsiveness of neural progenitors

We have previously found that acquisition of EGF responsiveness and expression of high levels of EGFR in neural progenitors of the GE is first observed at E18 (Ciccolini, 2001). We have also reported that GDF15 regulates EGFR expression in hippocampal neural progenitors (Carrillo-Garcia et al., 2014). Since the increase in *Gdf1*5 transcripts in the GE is temporally associated with acquisition of EGFR responsiveness, it is possible that GDF15 is involved in this transition. Therefore, we used immunofluorescence on coronal telencephalic sections to analyse total EGFR expression, i.e. intracellular and at the cell surface, in the VZ and SVZ of the GE of WT and Gdf15$^{-/-}$ E18 embryos. Qualitative analysis of the immunostained sections revealed a different organization of the EGFR^{+} cells. Whereas in the WT germinal epithelium they were mostly organised in columns of radially oriented cells (Fig. 4A white arrows), in the Gdf15$^{-/-}$ GE EGFR^{+} cells were associated in clusters (Fig. 4A). Additionally, the levels of fluorescence intensity relative to EGFR were lower across the whole V/SVZ of the mutant GE (Fig. 4B). Further confirming the change in EGFR levels, analysis of the dissociated tissue revealed a strong reduction in the number of cells displaying high levels of EGFR (E^{h}) at the cell membrane in the ganglionic eminence, independent of Prominin expression (supplementary Fig. S3). However, this reduction was significant only when EGFR was measured by binding of the less sensitive EGF-Alexa 488 (supplementary Fig. S3A, B) but not EGF-Alexa 647 (supplementary Fig. S3C, D), which unlike the first allows the detection of EGFR-expressing cells displaying also moderate levels of surface EGFR. Finally, analysis of *Egfr* transcripts in the two genotypes did not show any significant difference (supplementary Fig. S3E). As previously observed in the hippocampus (Carrillo-Garcia et al., 2014), in the WT and especially mutant GE (Fig. 4C and D, respectively), a short exposure to exogenous GDF15 promoted EGFR expression at the cells surface by a mechanism which required active CXCR4, as shown by the lower EGFR expression after treatment with CXCR4 antagonist AMD3100 (Fig. 4E). Taken together, these data show that GDF15 regulates cell surface EGFR expression in progenitors of the developing GE. We next asked if besides changes in EGFR expression, mutant progenitors differ from their WT counterpart in their ability to respond to EGF. For this, we first measured the ability of a short exposure to exogenous EGF to induce ERK phosphorylation in acutely dissociated cells from the E18 GE. This analysis revealed that independent of the

genotype, both cell groups similarly responded to EGF application (Supplementary Fig. S4A). Interestingly, a short application of GDF15 was also able to induce phosphorylation of ERK, consistent with the fact that it triggers GFRAL dependent signalling. However, the dynamic response to EGFR stimulation was affected by the genotype, since levels of phERK were significantly downregulated already one hour after EGF application in mutant but not WT cells (supplementary Fig. S4B) and a lower concentration of EGF was necessary to evoke a significant response in WT than in mutant cells (Supplementary Fig. S4C). Taken together, these data indicate that difference in EGFR levels between mutant and WT progenitors are associated with different activation dynamics in response to the growth factor.

We next examined whether these differences are reflected in the ability of EGF to affect proliferation *in situ*. We first investigated the relationship between cell proliferation and EGFR expression on coronal sections of the WT GE. For this analysis, we subdivided the GE in the three subregions as illustrated in Fig. 5A: the apical border (AB), the V/SVZ, i.e. the region including the two main germinal regions without the AB, and the GE outside of the germinal area containing more differentiated cells. Analysis of brain slices showed that independent of the genotype and the region, the vast majority of mitotic cells in the GE eminence was $EGFR^+$, again indicating that the genotype affects prominently levels of surface EGFR but not total EGFR (Fig. 5A, B). These findings also indicate a potential relevance of endogenous EGFR signalling in the regulation of proliferation. Indeed, pharmacological blockade of EGFR signalling with PD158780 (PD) reduced the number of cycling progenitors and drastically reduced mitosis at the apical and subapical side of the GE in both genotypes (Fig. 5C-E). However, the effect of the treatment on mitosis was significant in the mutant but not in the WT GE, likely reflecting the fact that in the WT GE the number of mitotic cells is low also in control conditions. On the contrary, independent of the genotype, exposing the dissected GE to exogenous EGF for 24 hours did not affect the number of cycling progenitors (Fig. 5C) and it led to a small but significant increase in the number of apically dividing cells in WT tissue and to a decrease in the number of apically dividing progenitors that was significant only in the subset of SAPs (Fig. 5D, E). Underscoring the difference of the effect of the treatment between the genotypes, exposure to exogenous EGF reduced the number of P^+ cells in the GE (Fig. 5F). Notably, this effect was only observed in the mutant tissue but not in the WT counterpart. Since GDF15 requires active CXCR4 signalling to modulate EGFR expression, and CXCR4 affects growth factor-dependent proliferation (Li et al., 2011), we next asked whether CXCR4 contributes to progenitor proliferation in the WT and mutant GE. Blockade of CXCR4 signalling by medium application of AMD3100 (AMD) led to a dramatic decrease in the number of cycling cells especially in WT mice (Fig. 5G). The treatment led to a significant decrease both in terms of total cycling cells and apically dividing progenitors in the WT and mutant tissue (Fig. 5G-I). Independent of the location, no mitotic cells could be observed in AMD treated WT tissue, whereas in the mutant tissue mitosis was significantly decreased only in apically dividing progenitors (Fig. 5H, I). Thus, unlike for the blockade of EGFR, blocking CXCR4 leads to a more dramatic outcome in the WT than in the mutant GE. This suggests that in the first EGFR signalling is more dependent on

CXCR4 activity than in the latter, which may reflect differences in EGFR expression between the two cell types. Supporting this conclusion, we found that independent of the genotype, blockade of CXCR4 affected especially the ability of EGFR^{high} progenitors to undergo clone formation (Fig. 5J). Taken together, these data show that EGFR signalling underlies the ability of apical GE progenitors to divide and that ablation of GDF15 affects EGFR expression, responsiveness and proliferation of apical progenitors.

GDF15 regulates the proliferation of intermediate progenitors in the developing GE

Cell cycle regulation affects neuronal output in the developing GE and in differentiating neurosphere cultures most immature neurons are generated from dividing progenitors (Ostenfeld and Svendsen, 2004; Suh et al., 2009). Therefore, we next used differentiating neurosphere cultures to begin to characterize the nature of the additionally proliferating cells in the absence of GDF15. Consistent with our previous observations *in vivo*, two days after induction of differentiation, Gdf15$^{-/-}$ neurosphere cultures contained significantly more cells replicating their DNA (Fig. 6A, B) and undergoing mitosis (Supplementary Fig. S5A, B) than their WT counterpart. This also resulted in a faster increase of Gdf15$^{-/-}$ cell culture confluence within the first 24h of plating (supplementary Fig. S5C). This difference could be prevented by adding exogenous GDF15 to the differentiation, but not proliferation, medium (Fig. 6B and data not shown). Moreover, this difference was transient as it was not observed when cultures were examined at later stages of differentiation (Fig. 6C) and could be rescued by addition of GDF15 to the differentiation medium (Fig. 6B, C). No difference in the number of pycnotic nuclei was observed in cultures that had been differentiating for two days (Supplementary Table S4), showing that the change in cell proliferation observed in mutant cultures was not due to an effect of GDF15 on cell death. However, cell viability was compromised in mutant cultures that had been differentiating for 4 days in the absence but not in the presence of exogenous GDF15 (Supplementary Table S5). Besides proliferation and cell viability the genotype also affected neuronal differentiation. After 7 days in differentiating conditions, neurospheres originating from the E18 WT GE gave rise to significantly more TuJ1^{+} neurons than the Gdf15$^{-/-}$ counterpart (Fig. 6D, E), whereas the number of O4^{+} cells was not affected by the genotype (supplementary Fig. S5D). Moreover, differences in the percentage of TuJ1^{+} neurons were not observed if cultures were allowed to differentiate for three further days (Fig. 6F) or if they were treated with exogenous GDF15. Taken together, these data indicate that lack of GDF15 although it increases the proliferation of neuronal progenitors it also affects their survival, leading to a transient increase in proliferation and a delay in neuronal differentiation. We next investigated changes in proliferation and neurogenesis *in vivo* in deeper areas of the GE tissue, containing differentiated neurons. Analysis 2 and 6 hours after BrdU injection showed a significant increase in the number of dividing cells only at the latter time point (Fig. 7A), suggesting that they may represent more slowly proliferating neuronal precursors. Consistent with this, the number of cells expressing MASH-1, which in the developing GE is necessary both for the proliferation and specification of neuronal progenitors (Casarosa et al., 1999; Torii et al., 1999) was higher in dissociated cells

obtained from the mutant E18 GE than in the tissue derived from their WT littermates (% immunopositive cells: WT = 22.84 ± 3.4; Gdf15$^{-/-}$ = 30.51 ± 2.2; P<0.05). A similar change was observed in the postnatal SVZ, where progenitors expressing MASH1 largely represent rapidly proliferating TAPs and pre-neuroblasts (Cesetti et al., 2009; Parras et al., 2004). In the postnatal ventral and mediolateral portion of the V/SVZ MASH1^{+} progenitors were more abundant in Gdf15$^{-/-}$ than in WT mice (Fig. 7B, C). Moreover, this increase was limited to the fraction of MASH1^{+}/Ki67^{+} proliferating progenitors (Fig. 7C) and was not observed at the level of the dorsolateral corner (Fig. 7D). A subset of MASH1^{+} cells, but not pre-neuroblasts, also express Olig2, a helix-loop helix transcription factor associated to oligodendrocyte differentiation (Cesetti et al., 2009; Lu et al., 2002; Zhou and Anderson, 2002). We therefore next analysed the expression of Olig2 by immunohistofluorescence in the WT and Gdf15$^{-/-}$ mediolateral V/SVZ. Independent of MASH1 expression, the number of Olig2^{+} cells was not affected by the genotype (supplementary Fig. S6A). Likewise, we did not detect differences between total or proliferating DCX^{+}/Ki67^{+} neuroblasts (Supplementary Fig. S6B, C) between the WT and mutant V/SVZ. We next investigated if cell death was also increased *in vivo* in the absence of GDF15, as this could explain why the extra-proliferating MASH1^{+} progenitors in the Gdf15$^{-/-}$ V/SVZ do not give rise to a higher number of postmitotic neuroblasts in the V/SVZ. Indeed, analysis by flow cytometry showed that, compared to the WT, the percentage of PI^{+} (i.e., dead) cells was higher in both populations in the mutant V/SVZ (EGFR^{high} cells: fold increase 2.00 ± 0.3382; p = 0.0369; EGFR^{low} cells: fold increase 1.380 ± 0.1094; p = 0.0511) and Annexin V positive cells were increased in mutant brain slices (Supplementary Fig. S6D). Taken together, our data indicate that both *in vitro* and *in vivo*, the increase in proliferation of mutant neuronal progenitors does not lead to increased neurogenesis, likely due to compensatory cell death.

GDF15 regulates the number of NSCs and ependymal cells

Apically dividing progenitors in the developing GE will give rise to ependymal and adult NSCs, which to a great extent derive from a common progenitor undergoing proliferation around mid-development (Ortiz-Alvarez et al., 2019) by a mechanism that involves BMP-mediated control of cell cycle regulators (Omiya et al., 2021). Moreover, both apical NSCs and ependymal cells continue to express Prominin in the postnatal SVZ (Baur et al., 2022; Carrillo-Garcia et al., 2010; Khatri et al., 2014). Therefore, we next investigated whether the increase in the proliferation of apically dividing progenitors also affects the generation of these cell types by examining the effect of the genotype on the number of multiciliated ependymal cells and progenitors displaying only one primary cilium at the apical surface of new-born mice at postnatal day 2 (P2). This analysis revealed a significant increase in multiciliated ependymal as well as a trend increase in single-ciliated (SC) cells in the mutant tissue compared to the WT counterpart and a significant increase in the number of total cells (Fig. 8A-C). Consistent with that, we found that the number of both ependymal cells and non-ependymal GFAP expressing apical NSCs was increased in the adult V/SVZ, when ependymal cells are fully differentiated (Fig. 8D, E). We next investigated whether besides NSCs, activated NSCs

are also increased in the mutant adult V/SVZ. For this we examined the number of cells expressing high levels of EGFR in the V/SVZ of adult mutant and WT mice as described before (Carrillo-Garcia et al., 2010; Khatri et al., 2014). This analysis revealed that both P^-E^h and P^+E^h double positive cells were increased in the V/SVZ of $Gdf15^{-/-}$ adult mice (Fig. 8F) and the incidence of clonogenic cells was not affected by the genotype (Supplementary Table S6), showing that total NSCs are increased in the absence of GDF15. Together, these data indicate that lack of GDF15 increases the number of both cell types by increasing proliferation of apical progenitors rather than biasing their differentiation. Thus, our data demonstrate that GDF15 controls the number of ependymal and NSCs in the adult SVZ, by regulating proliferation of apically dividing embryonic progenitors.

Discussion

GDF15 is a member of the TGF-β superfamily with largely unknown functions. Earlier studies indicated that the neonatal periventricular zone and the choroid plexus are the main sources of GDF15 within the brain (Bottner et al., 1999; Schober et al., 2001). Further supporting a role for GDF15 in the developing periventricular germinal zone, we show that GDF15 is expressed in apical and basal progenitors of the embryonic GE and in the adult V/SVZ, which largely derives from the first. Most importantly, our data provide first evidence that in these regions, GDF15 plays a role in the regulation of growth factor responsiveness, cell cycle kinetics and cell survival ultimately regulating the number of adult NSCs.

Previous studies have shown that most ependymal cells are born during mid late development and although becoming postmitotic they differentiate only after birth (Redmond et al., 2019; Spassky et al., 2005). Around the same time, NSCs begin a transition into quiescence, which continues into the early postnatal weeks (Borrett et al., 2020; Fuentealba et al., 2015; Furutachi et al., 2015). The generation of ependymal cells and NSCs is linked as they share a common progenitor (Ortiz-Alvarez et al., 2019). Our analysis focuses here on the effect of GDF15 on apical NSCs, which we have recently shown represent a minor pool of NSCs in the adult V/SVZ are characterized by Prominin-1 expression and display an apical membrane and a primary cilium (Baur et al., 2022). Since basal NSCs likely derive from apical NSCs (Obernier et al., 2018), it is possible that also the number of the latter will be increased in the absence of GDF15, however this issue remains to be investigated.

The increase of GDF15 expression at late stages of development is suggestive of a developmental role for the growth factor in the regulation of the number of common progenitors and underscores a striking temporal correlation between the increase in GDF15, changes in cell cycle dynamics and in EGFR expression observed during development affecting multiple aspects of neural progenitor behaviour including proliferation (Burrows et al., 1997; Ciccolini and Svendsen, 1998; Craig et al., 1996; Gritti et al., 1999; Suh et al., 2009), migration (Aguirre et al., 2005; Caric et al., 2001; Ciccolini et al., 2005), differentiation (Ivkovic et al., 2008), and survival by activating multiple downstream pathways (Cochard et al., 2021). Supporting a role for GDF15 in orchestrating these developmental changes we found that short exposure to exogenous

GDF15 reduces progenitor proliferation and rescues EGFR expression, showing that the phenotype observed in the mutant V/SVZ is not the result of a selective process.

At a cellular level we found that GDF15 affects proliferation by decreasing the pool of cycling cells and slowing cell cycle progression. However, GDF15 is not required for the extra generated cells to permanently exit the cell cycle and differentiate. Instead, our data *in vitro* and *in vivo* support the notion that while extra progenitor cells are generated both in the VZ and in the SVZ they will proceed to differentiate in a normal manner leading to the generation of extra progenitors that in the VZ will give rise to extra numerary ependymal cells and NSCs and ependymal cells, whereas in the VSZ to neuronal progenitors that will undergo compensatory cell death. Compensatory cell death was also observed upon increase of neural progenitor proliferation following loss of mCD24 expression (Belvindrah et al., 2002), suggesting that it may represent a common route of regulation of neurogenesis in the postnatal niche. However, in the mutant embryonic GE, the increase in the number of $MASH1^{+}$ cells was not associated to extra cell death. Since many of the cells generated at E18 in the GE migrate away and undergo terminal differentiation in the dorsal telencephalon, it is possible that the supernumerary cells generated in the $Gdf15^{-/-}$ GE eventually undergo compensatory cell death in other regions of the telencephalon and therefore escaped our analysis. Interestingly, the increase in GDF15 expression coincides with the time that apical RG progenitors start to withdraw from cell cycle and transition to the state of quiescent adult NSCs. Gene signature analysis have revealed that this transition involves shutting down several biological processes occurring between E17 and postnatal day P6 (Borrett et al., 2020), and that upon reactivation, adult NSCs reacquire characteristics of RG. Indeed, we here found that upon activation adult NSCs display the same increase in cell cycle kinetics as observed in embryonic progenitors.

Our data indicate that at the molecular level GDF15 may affect at least in part the proliferation of apical progenitors by modulating EGFR expression. Indeed, a brief exposure to exogenous GDF15 reversed the defect in EGFR expression and modulation of EGFR signalling affected the proliferation and number of apical progenitors. From late developments onwards, EGFR expression is also upregulated in NSCs and progenitor cells and EGF is the main mitogen for NSCs (Cesetti et al., 2009; Ciccolini, 2001). We here show a close association between EGFR expression and proliferation also *in vivo*, as independent of the genotype most mitotic cells expressed EGFR. Moreover, our data indicate that levels of EGFR expression affect the proliferative response to EGF, as mutant progenitors appear more dependent on endogenous EGFR signalling to undergo fast proliferation whereas activation of EGFR had opposite effects in mutant and WT GE progenitors. That EGFR signalling is an important component of the regulation of apical progenitors is consistent with observation that in rodents, EGFR ligands are a constant component of the cerebrospinal fluid (Van Setten et al., 1999). Moreover, at late developmental stages in the rat telencephalon TGFα is highly expressed in the choroid plexus and in the differentiated portion of GE (Kornblum et al., 1997), indicating a maximal availability of EGFR ligands at the apical and basal border of the VZ and SVZ, respectively. Consistent with the regional expression of EGFR ligands, in the postnatal brain EGFR activation is crucial for the regulation of the

differentiation of ependymal cells from RG progenitors (Abdi et al., 2019). Although our data indicate that GDF15 affects the proliferation of a common ependymal/NSC progenitor likely by altering EGFR expression, we did not observe a bias in differentiation, in line with the fact that EGFR impinges on multiple pathways (Cochard et al., 2021). Interestingly, embryonic human NSCs also overexpress GDF15 (Wang et al., 2010) and EGF is present in the human cerebrospinal fluid (Godard et al., 2003; Shnaper et al., 2009). Thus, our observation may have a potential relevance for the regulation of proliferation in human NSCs.

References

Abdi, K., Neves, G., Pyun, J., Kiziltug, E., Ahrens, A., Kuo, C.T., 2019. EGFR Signaling Termination via Numb Trafficking in Ependymal Progenitors Controls Postnatal Neurogenic Niche Differentiation. Cell Rep 28, 2012-2022 e2014.

Aguirre, A., Rizvi, T.A., Ratner, N., Gallo, V., 2005. Overexpression of the epidermal growth factor receptor confers migratory properties to nonmigratory postnatal neural progenitors. J Neurosci 25, 11092-11106.

Baur, K., Abdullah, Y., Mandl, C., Holzl-Wenig, G., Shi, Y., Edelkraut, U., Khatri, P., Hagenston, A.M., Irmler, M., Beckers, J., Ciccolini, F., 2022. A novel stem cell type at the basal side of the subventricular zone maintains adult neurogenesis. EMBO Rep, e54078.

Belvindrah, R., Rougon, G., Chazal, G., 2002. Increased neurogenesis in adult mCD24-deficient mice. J Neurosci 22, 3594-3607.

Bittman, K., Owens, D.F., Kriegstein, A.R., LoTurco, J.J., 1997. Cell coupling and uncoupling in the ventricular zone of developing neocortex. J Neurosci 17, 7037-7044.

Borrett, M.J., Innes, B.T., Jeong, D., Tahmasian, N., Storer, M.A., Bader, G.D., Kaplan, D.R., Miller, F.D., 2020. Single-Cell Profiling Shows Murine Forebrain Neural Stem Cells Reacquire a Developmental State when Activated for Adult Neurogenesis. Cell Rep 32, 108022.

Bottner, M., Suter-Crazzolara, C., Schober, A., Unsicker, K., 1999. Expression of a novel member of the TGF-beta superfamily, growth/differentiation factor-15/macrophage-inhibiting cytokine-1 (GDF-15/MIC-1) in adult rat tissues. Cell Tissue Res 297, 103-110.

Burrows, R.C., Wancio, D., Levitt, P., Lillien, L., 1997. Response diversity and the timing of progenitor cell maturation are regulated by developmental changes in EGFR expression in the cortex. Neuron 19, 251-267.

Calegari, F., Haubensak, W., Haffner, C., Huttner, W.B., 2005. Selective lengthening of the cell cycle in the neurogenic subpopulation of neural progenitor cells during mouse brain development. J Neurosci 25, 6533-6538.

Caric, D., Raphael, H., Viti, J., Feathers, A., Wancio, D., Lillien, L., 2001. EGFRs mediate chemotactic migration in the developing telencephalon. Development 128, 4203-4216.

Carrillo-Garcia, C., Prochnow, S., Simeonova, I.K., Strelau, J., Hölzl-Wenig, G., Mandl, C., Unsicker, K., von Bohlen Und Halbach, O., Ciccolini, F., 2014. Growth/differentiation factor 15 promotes EGFR signalling, and regulates proliferation and migration in the hippocampus of neonatal and young adult mice. Development 141, 773-783.

Carrillo-Garcia, C., Suh, Y., Obernier, K., Holzl-Wenig, G., Mandl, C., Ciccolini, F., 2010. Multipotent precursors in the anterior and hippocampal subventricular zone

display similar transcription factor signatures but their proliferation and maintenance are differentially regulated. Mol Cell Neurosci 44, 318-329.
Casarosa, S., Fode, C., Guillemot, F., 1999. Mash1 regulates neurogenesis in the ventral telencephalon. Development 126, 525-534.
Cesetti, T., Obernier, K., Bengtson, C.P., Fila, T., Mandl, C., Holzl-Wenig, G., Worner, K., Eckstein, V., Ciccolini, F., 2009. Analysis of stem cell lineage progression in the neonatal subventricular zone identifies EGFR+/NG2- cells as transit-amplifying precursors. Stem Cells 27, 1443-1454.
Chenn, A., McConnell, S.K., 1995. Cleavage orientation and the asymmetric inheritance of Notch1 immunoreactivity in mammalian neurogenesis. Cell 82, 631-641.
Ciccolini, F., 2001. Identification of two distinct types of multipotent neural precursors that appear sequentially during CNS development. Mol Cell Neurosci 17, 895-907.
Ciccolini, F., Mandl, C., Holzl-Wenig, G., Kehlenbach, A., Hellwig, A., 2005. Prospective isolation of late development multipotent precursors whose migration is promoted by EGFR. Dev Biol 284, 112-125.
Ciccolini, F., Svendsen, C.N., 1998. Fibroblast growth factor 2 (FGF-2) promotes acquisition of epidermal growth factor (EGF) responsiveness in mouse striatal precursor cells: identification of neural precursors responding to both EGF and FGF-2. J Neurosci 18, 7869-7880.
Ciccolini, F., Svendsen, C.N., 2001. Neurotrophin responsiveness is differentially regulated in neurons and precursors isolated from the developing striatum. J Mol Neurosci 17, 25-33.
Cochard, L.M., Levros, L.C., Jr., Joppe, S.E., Pratesi, F., Aumont, A., Fernandes, K.J.L., 2021. Manipulation of EGFR-Induced Signaling for the Recruitment of Quiescent Neural Stem Cells in the Adult Mouse Forebrain. Front Neurosci 15, 621076.
Craig, C.G., Tropepe, V., Morshead, C.M., Reynolds, B.A., Weiss, S., van der Kooy, D., 1996. In vivo growth factor expansion of endogenous subependymal neural precursor cell populations in the adult mouse brain. J Neurosci 16, 2649-2658.
Culican, S.M., Baumrind, N.L., Yamamoto, M., Pearlman, A.L., 1990. Cortical radial glia: identification in tissue culture and evidence for their transformation to astrocytes. J Neurosci 10, 684-692.
Dause, T.J., Denninger, J.K., Smith, B.M., Kirby, E.D., 2022. The neural stem cell secretome across neurodevelopment. Exp Neurol 355, 114142.
Englund, C., Fink, A., Lau, C., Pham, D., Daza, R.A., Bulfone, A., Kowalczyk, T., Hevner, R.F., 2005. Pax6, Tbr2, and Tbr1 are expressed sequentially by radial glia, intermediate progenitor cells, and postmitotic neurons in developing neocortex. J Neurosci 25, 247-251.
Falk, S., Bugeon, S., Ninkovic, J., Pilz, G.A., Postiglione, M.P., Cremer, H., Knoblich, J.A., Gotz, M., 2017. Time-Specific Effects of Spindle Positioning on Embryonic Progenitor Pool Composition and Adult Neural Stem Cell Seeding. Neuron 93, 777-791 e773.
Fuentealba, L.C., Rompani, S.B., Parraguez, J.I., Obernier, K., Romero, R., Cepko, C.L., Alvarez-Buylla, A., 2015. Embryonic Origin of Postnatal Neural Stem Cells. Cell 161, 1644-1655.
Furutachi, S., Miya, H., Watanabe, T., Kawai, H., Yamasaki, N., Harada, Y., Imayoshi, I., Nelson, M., Nakayama, K.I., Hirabayashi, Y., Gotoh, Y., 2015. Slowly dividing neural progenitors are an embryonic origin of adult neural stem cells. Nat Neurosci 18, 657-665.
Gakhar-Koppole, N., Hundeshagen, P., Mandl, C., Weyer, S.W., Allinquant, B., Muller, U., Ciccolini, F., 2008. Activity requires soluble amyloid precursor protein alpha to

promote neurite outgrowth in neural stem cell-derived neurons via activation of the MAPK pathway. Eur J Neurosci 28, 871-882.
Godard, S., Getz, G., Delorenzi, M., Farmer, P., Kobayashi, H., Desbaillets, I., Nozaki, M., Diserens, A.C., Hamou, M.F., Dietrich, P.Y., Regli, L., Janzer, R.C., Bucher, P., Stupp, R., de Tribolet, N., Domany, E., Hegi, M.E., 2003. Classification of human astrocytic gliomas on the basis of gene expression: a correlated group of genes with angiogenic activity emerges as a strong predictor of subtypes. Cancer Res 63, 6613-6625.
Gritti, A., Frolichsthal-Schoeller, P., Galli, R., Parati, E.A., Cova, L., Pagano, S.F., Bjornson, C.R., Vescovi, A.L., 1999. Epidermal and fibroblast growth factors behave as mitogenic regulators for a single multipotent stem cell-like population from the subventricular region of the adult mouse forebrain. J Neurosci 19, 3287-3297.
Hartfuss, E., Galli, R., Heins, N., Gotz, M., 2001. Characterization of CNS precursor subtypes and radial glia. Dev Biol 229, 15-30.
Haubensak, W., Attardo, A., Denk, W., Huttner, W.B., 2004. Neurons arise in the basal neuroepithelium of the early mammalian telencephalon: a major site of neurogenesis. Proc Natl Acad Sci U S A 101, 3196-3201.
Huttner, W.B., Kosodo, Y., 2005. Symmetric versus asymmetric cell division during neurogenesis in the developing vertebrate central nervous system. Curr Opin Cell Biol 17, 648-657.
Ivkovic, S., Canoll, P., Goldman, J.E., 2008. Constitutive EGFR signaling in oligodendrocyte progenitors leads to diffuse hyperplasia in postnatal white matter. J Neurosci 28, 914-922.
Kefaloyianni, E., Muthu, M.L., Kaeppler, J., Sun, X., Sabbisetti, V., Chalaris, A., Rose-John, S., Wong, E., Sagi, I., Waikar, S.S., Rennke, H., Humphreys, B.D., Bonventre, J.V., Herrlich, A., 2016. ADAM17 substrate release in proximal tubule drives kidney fibrosis. JCI Insight 1.
Kelly, S.M., Raudales, R., He, M., Lee, J.H., Kim, Y., Gibb, L.G., Wu, P., Matho, K., Osten, P., Graybiel, A.M., Huang, Z.J., 2018. Radial Glial Lineage Progression and Differential Intermediate Progenitor Amplification Underlie Striatal Compartments and Circuit Organization. Neuron 99, 345-361 e344.
Khatri, P., Obernier, K., Simeonova, I.K., Hellwig, A., Hölzl-Wenig, G., Mandl, C., Scholl, C., Wolfl, S., Winkler, J., Gaspar, J.A., Sachinidis, A., Ciccolini, F., 2014. Proliferation and cilia dynamics in neural stem cells prospectively isolated from the SEZ. Sci Rep 4, 3803.
Kornblum, H.I., Hussain, R.J., Bronstein, J.M., Gall, C.M., Lee, D.C., Seroogy, K.B., 1997. Prenatal ontogeny of the epidermal growth factor receptor and its ligand, transforming growth factor alpha, in the rat brain. J Comp Neurol 380, 243-261.
Kosodo, Y., Huttner, W.B., 2009. Basal process and cell divisions of neural progenitors in the developing brain. Dev Growth Differ 51, 251-261.
Kosodo, Y., Roper, K., Haubensak, W., Marzesco, A.M., Corbeil, D., Huttner, W.B., 2004. Asymmetric distribution of the apical plasma membrane during neurogenic divisions of mammalian neuroepithelial cells. EMBO J 23, 2314-2324.
Levitt, P., Rakic, P., 1980. Immunoperoxidase localization of glial fibrillary acidic protein in radial glial cells and astrocytes of the developing rhesus monkey brain. J Comp Neurol 193, 815-840.
Li, F., Ruan, X., Min, L., 2017. Targeting both sides of the GDF15-GFRAL-RET receptor complex: A new approach to achieve body weight homeostasis. Genes Dis 4, 183-184.

Li, M., Chang, C.J., Lathia, J.D., Wang, L., Pacenta, H.L., Cotleur, A., Ransohoff, R.M., 2011. Chemokine receptor CXCR4 signaling modulates the growth factor-induced cell cycle of self-renewing and multipotent neural progenitor cells. Glia 59, 108-118.
LoTurco, J.J., Blanton, M.G., Kriegstein, A.R., 1991. Initial expression and endogenous activation of NMDA channels in early neocortical development. J Neurosci 11, 792-799.
Lu, Q.R., Sun, T., Zhu, Z., Ma, N., Garcia, M., Stiles, C.D., Rowitch, D.H., 2002. Common developmental requirement for Olig function indicates a motor neuron/oligodendrocyte connection. Cell 109, 75-86.
Matsushima, A., Graybiel, A.M., 2020. Combinatorial Developmental Controls on Striatonigral Circuits. Cell Rep 31, 107778.
McKay, R., 1997. Stem cells in the central nervous system. Science 276, 66-71.
Merkle, F.T., Tramontin, A.D., Garcia-Verdugo, J.M., Alvarez-Buylla, A., 2004. Radial glia give rise to adult neural stem cells in the subventricular zone. Proc Natl Acad Sci U S A 101, 17528-17532.
Misson, J.P., Edwards, M.A., Yamamoto, M., Caviness, V.S., Jr., 1988. Identification of radial glial cells within the developing murine central nervous system: studies based upon a new immunohistochemical marker. Brain Res Dev Brain Res 44, 95-108.
Mullican, S.E., Lin-Schmidt, X., Chin, C.N., Chavez, J.A., Furman, J.L., Armstrong, A.A., Beck, S.C., South, V.J., Dinh, T.Q., Cash-Mason, T.D., Cavanaugh, C.R., Nelson, S., Huang, C., Hunter, M.J., Rangwala, S.M., 2017. GFRAL is the receptor for GDF15 and the ligand promotes weight loss in mice and nonhuman primates. Nat Med 23, 1150-1157.
Noctor, S.C., Flint, A.C., Weissman, T.A., Dammerman, R.S., Kriegstein, A.R., 2001. Neurons derived from radial glial cells establish radial units in neocortex. Nature 409, 714-720.
Noctor, S.C., Martinez-Cerdeno, V., Ivic, L., Kriegstein, A.R., 2004. Cortical neurons arise in symmetric and asymmetric division zones and migrate through specific phases. Nat Neurosci 7, 136-144.
Noctor, S.C., Martinez-Cerdeno, V., Kriegstein, A.R., 2008. Distinct behaviors of neural stem and progenitor cells underlie cortical neurogenesis. J Comp Neurol 508, 28-44.
Obernier, K., Cebrian-Silla, A., Thomson, M., Parraguez, J.I., Anderson, R., Guinto, C., Rodas Rodriguez, J., Garcia-Verdugo, J.M., Alvarez-Buylla, A., 2018. Adult Neurogenesis Is Sustained by Symmetric Self-Renewal and Differentiation. Cell Stem Cell 22, 221-234 e228.
Omiya, H., Yamaguchi, S., Watanabe, T., Kuniya, T., Harada, Y., Kawaguchi, D., Gotoh, Y., 2021. BMP signaling suppresses Gemc1 expression and ependymal differentiation of mouse telencephalic progenitors. Sci Rep 11, 613.
Ortiz-Alvarez, G., Daclin, M., Shihavuddin, A., Lansade, P., Fortoul, A., Faucourt, M., Clavreul, S., Lalioti, M.E., Taraviras, S., Hippenmeyer, S., Livet, J., Meunier, A., Genovesio, A., Spassky, N., 2019. Adult Neural Stem Cells and Multiciliated Ependymal Cells Share a Common Lineage Regulated by the Geminin Family Members. Neuron 102, 159-172 e157.
Ostenfeld, T., Svendsen, C.N., 2004. Requirement for neurogenesis to proceed through the division of neuronal progenitors following differentiation of epidermal growth factor and fibroblast growth factor-2-responsive human neural stem cells. Stem Cells 22, 798-811.
Parras, C.M., Galli, R., Britz, O., Soares, S., Galichet, C., Battiste, J., Johnson, J.E., Nakafuku, M., Vescovi, A., Guillemot, F., 2004. Mash1 specifies neurons and oligodendrocytes in the postnatal brain. EMBO J 23, 4495-4505.

Petros, T.J., Bultje, R.S., Ross, M.E., Fishell, G., Anderson, S.A., 2015. Apical versus Basal Neurogenesis Directs Cortical Interneuron Subclass Fate. Cell Rep 13, 1090-1095.
Pilz, G.A., Shitamukai, A., Reillo, I., Pacary, E., Schwausch, J., Stahl, R., Ninkovic, J., Snippert, H.J., Clevers, H., Godinho, L., Guillemot, F., Borrell, V., Matsuzaki, F., Götz, M., 2013. Amplification of progenitors in the mammalian telencephalon includes a new radial glial cell type. Nat Commun 4, 2125.
Rakic, P., 1972. Mode of cell migration to the superficial layers of fetal monkey neocortex. J Comp Neurol 145, 61-83.
Redmond, S.A., Figueres-Onate, M., Obernier, K., Nascimento, M.A., Parraguez, J.I., Lopez-Mascaraque, L., Fuentealba, L.C., Alvarez-Buylla, A., 2019. Development of Ependymal and Postnatal Neural Stem Cells and Their Origin from a Common Embryonic Progenitor. Cell Rep 27, 429-441 e423.
Schindelin, J., Arganda-Carreras, I., Frise, E., Kaynig, V., Longair, M., Pietzsch, T., Preibisch, S., Rueden, C., Saalfeld, S., Schmid, B., Tinevez, J.Y., White, D.J., Hartenstein, V., Eliceiri, K., Tomancak, P., Cardona, A., 2012. Fiji: an open-source platform for biological-image analysis. Nat Methods 9, 676-682.
Schober, A., Bottner, M., Strelau, J., Kinscherf, R., Bonaterra, G.A., Barth, M., Schilling, L., Fairlie, W.D., Breit, S.N., Unsicker, K., 2001. Expression of growth differentiation factor-15/ macrophage inhibitory cytokine-1 (GDF-15/MIC-1) in the perinatal, adult, and injured rat brain. J Comp Neurol 439, 32-45.
Shnaper, S., Desbaillets, I., Brown, D.A., Murat, A., Migliavacca, E., Schluep, M., Ostermann, S., Hamou, M.F., Stupp, R., Breit, S.N., de Tribolet, N., Hegi, M.E., 2009. Elevated levels of MIC-1/GDF15 in the cerebrospinal fluid of patients are associated with glioblastoma and worse outcome. Int J Cancer 125, 2624-2630.
Spassky, N., Han, Y.G., Aguilar, A., Strehl, L., Besse, L., Laclef, C., Ros, M.R., Garcia-Verdugo, J.M., Alvarez-Buylla, A., 2008. Primary cilia are required for cerebellar development and Shh-dependent expansion of progenitor pool. Dev Biol 317, 246-259.
Spassky, N., Merkle, F.T., Flames, N., Tramontin, A.D., Garcia-Verdugo, J.M., Alvarez-Buylla, A., 2005. Adult ependymal cells are postmitotic and are derived from radial glial cells during embryogenesis. J Neurosci 25, 10-18.
Stancik, E.K., Navarro-Quiroga, I., Sellke, R., Haydar, T.F., 2010. Heterogeneity in ventricular zone neural precursors contributes to neuronal fate diversity in the postnatal neocortex. J Neurosci 30, 7028-7036.
Strelau, J., Schmeer, C., Peterziel, H., Sackmann, T., Herold-Mende, C., Steiner, H., Weller, M., Unsicker, K., 2008. Expression and putative functions of GDF-15, a member of the TGF-beta superfamily, in human glioma and glioblastoma cell lines. Cancer Lett 270, 30-39.
Strelau, J., Strzelczyk, A., Rusu, P., Bendner, G., Wiese, S., Diella, F., Altick, A.L., von Bartheld, C.S., Klein, R., Sendtner, M., Unsicker, K., 2009. Progressive postnatal motoneuron loss in mice lacking GDF-15. J Neurosci 29, 13640-13648.
Suh, Y., Obernier, K., Holzl-Wenig, G., Mandl, C., Herrmann, A., Worner, K., Eckstein, V., Ciccolini, F., 2009. Interaction between DLX2 and EGFR regulates proliferation and neurogenesis of SVZ precursors. Mol Cell Neurosci 42, 308-314.
Tan, X., Liu, W.A., Zhang, X.J., Shi, W., Ren, S.Q., Li, Z., Brown, K.N., Shi, S.H., 2016. Vascular Influence on Ventral Telencephalic Progenitors and Neocortical Interneuron Production. Dev Cell 36, 624-638.
Torii, M., Matsuzaki, F., Osumi, N., Kaibuchi, K., Nakamura, S., Casarosa, S., Guillemot, F., Nakafuku, M., 1999. Transcription factors Mash-1 and Prox-1 delineate early steps in differentiation of neural stem cells in the developing central nervous system. Development 126, 443-456.

Tyler, W.A., Haydar, T.F., 2013. Multiplex genetic fate mapping reveals a novel route of neocortical neurogenesis, which is altered in the Ts65Dn mouse model of Down syndrome. J Neurosci 33, 5106-5119.

Van Setten, G.B., Edstrom, L., Stibler, H., Rasmussen, S., Schultz, G., 1999. Levels of transforming growth factor alpha (TGF-alpha) in human cerebrospinal fluid. Int J Dev Neurosci 17, 131-134.

Voigt, T., 1989. Development of glial cells in the cerebral wall of ferrets: direct tracing of their transformation from radial glia into astrocytes. J Comp Neurol 289, 74-88.

Wang, F., Guo, Y., Yu, H., Zheng, L., Mi, L., Gao, W., 2010. Growth differentiation factor 15 in different stages of heart failure: potential screening implications. Biomarkers 15, 671-676.

Yang, L., Chang, C.C., Sun, Z., Madsen, D., Zhu, H., Padkjaer, S.B., Wu, X., Huang, T., Hultman, K., Paulsen, S.J., Wang, J., Bugge, A., Frantzen, J.B., Norgaard, P., Jeppesen, J.F., Yang, Z., Secher, A., Chen, H., Li, X., John, L.M., Shan, B., He, Z., Gao, X., Su, J., Hansen, K.T., Yang, W., Jorgensen, S.B., 2017. GFRAL is the receptor for GDF15 and is required for the anti-obesity effects of the ligand. Nat Med 23, 1158-1166.

Zhang, R., Zhang, Z., Zhang, C., Zhang, L., Robin, A., Wang, Y., Lu, M., Chopp, M., 2004. Stroke transiently increases subventricular zone cell division from asymmetric to symmetric and increases neuronal differentiation in the adult rat. J Neurosci 24, 5810-5815.

Zhou, Q., Anderson, D.J., 2002. The bHLH transcription factors OLIG2 and OLIG1 couple neuronal and glial subtype specification. Cell 109, 61-73.

Tables and Figures

Table 1: Extra BrdU incorporating cells exit the cell cycle in the *Gdf15*$^{-/-}$ GE after cell division

Quantitative analysis of the percentage of BrdU^{+} that are still cycling (BrdU^{+}/Ki67^{+}) or have exited the cell cycle (BrdU^{+}/Ki67^{-}) within the germinal (VZ/SVZ) and the differentiated region of the GE (GE) of E18 WT and *Gdf15*$^{-/-}$ embryos 6 hours after BrdU injection.

	WT		*Gdf15*$^{-/-}$	
	V/SVZ	GE	V/SVZ	GE
Brdu^{+}/Ki67^{-} (% BrdU^{+})	23.9 ± 2.8	22.3± 1.0	42.5 ± 4.3**	32.6± 3.6*
Brdu^{+}/Ki67^{+} (% BrdU^{+})	76.0± 2.8	77.6± 1.5	57.4± 4.3**	67.3± 3.0*

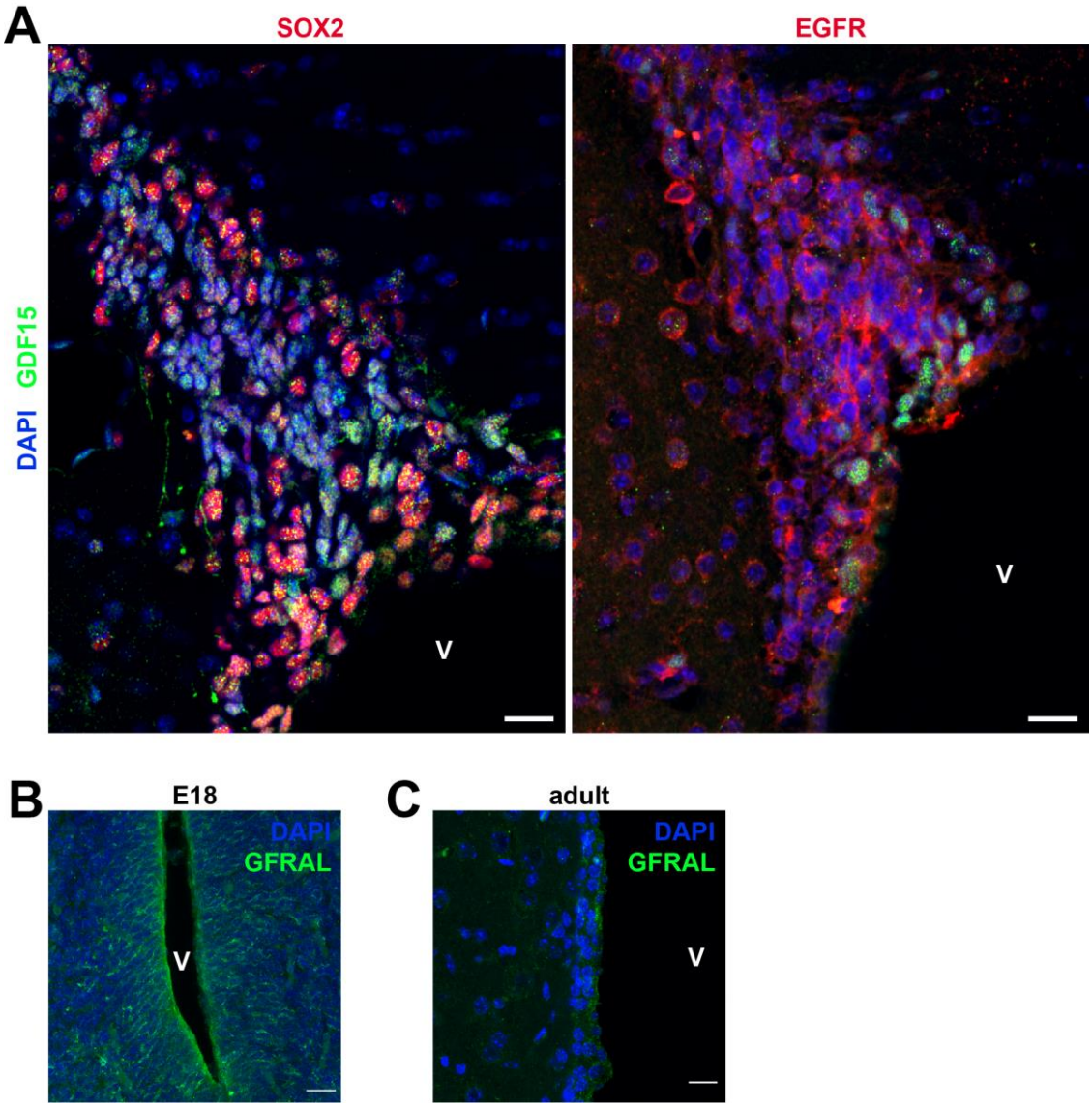

Figure 1: GDF15 and its receptor GFRAL are expressed in the V/SVZ.
(A) Immunofluorescent staining of brain slices from 8w-old mice for GDF15 (green) and either Sox2 or EGFR (red). DAPI was used as nuclear counterstain. V= ventricle; scale bar = 20 µm.
(B, C) Immunofluorescent staining of brain slices from E18 (B) or 8w-old mice (C) for GFRAL (green). DAPI was used as nuclear counterstain. V= ventricle; scale bar = 20 µm.

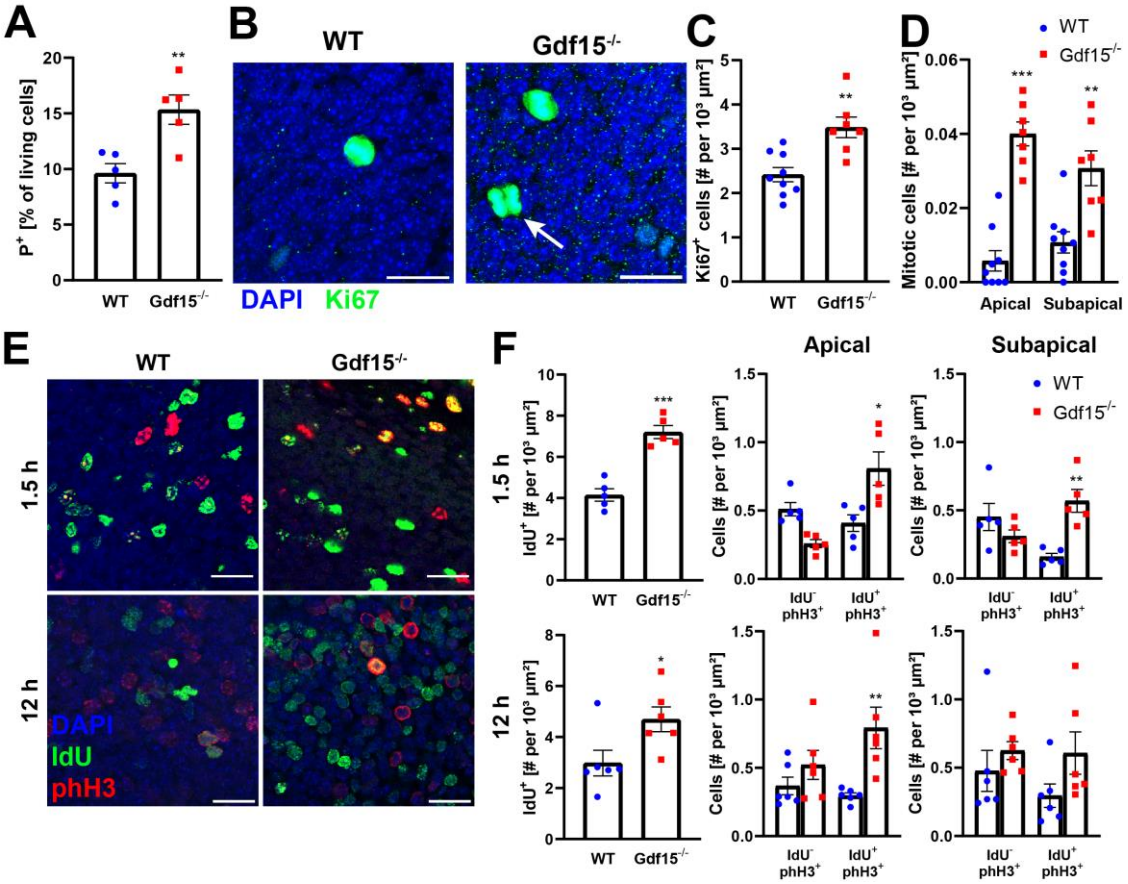

Figure 2: Gdf15$^{-/-}$ mice display increased proliferation and number of proliferating cells in the VZ of the embryonic GE.

(A) Percentage of Prominin-expressing cells in the E18 GE of wild-type (WT) and Gdf15$^{-/-}$ mice analysed by flow cytometry.

(B) Immunofluorescent staining of E18 GE whole mounts for proliferation marker Ki67 (green). Confocal images are taken at the apical side of the GE. DAPI was used as nuclear counterstain. White arrow indicates a mitotic cell. V= ventricle; scale bar = 20 µm.

(C, D) Quantification of total number of Ki67^{+} cells (C) and mitotic cells in the apical and subapical cell layers (D) in E18 whole mounts.

(E) Immunofluorescent staining of E18 GE whole mounts for proliferation marker phH3 (red) and IdU (green). Images are taken at the apical side of the GE. The dissected tissue was incubated in IdU for 1.5h and directly fixed, or further incubated without IdU for 12h. DAPI was used as nuclear counterstain. Scale bars = 20 µm.

(F) Quantification of cells labelled with IdU and phH3 directly after IdU application (1.5h) or after a 12h chase period (12h). Cells expressing phH3 were counted separately depending on location of the nucleus (apical or subapical) to infer the type of progenitor.

Bars represent mean ± SEM; * indicate significance: *p<0.05, **p<0.01, ***p<0.001.

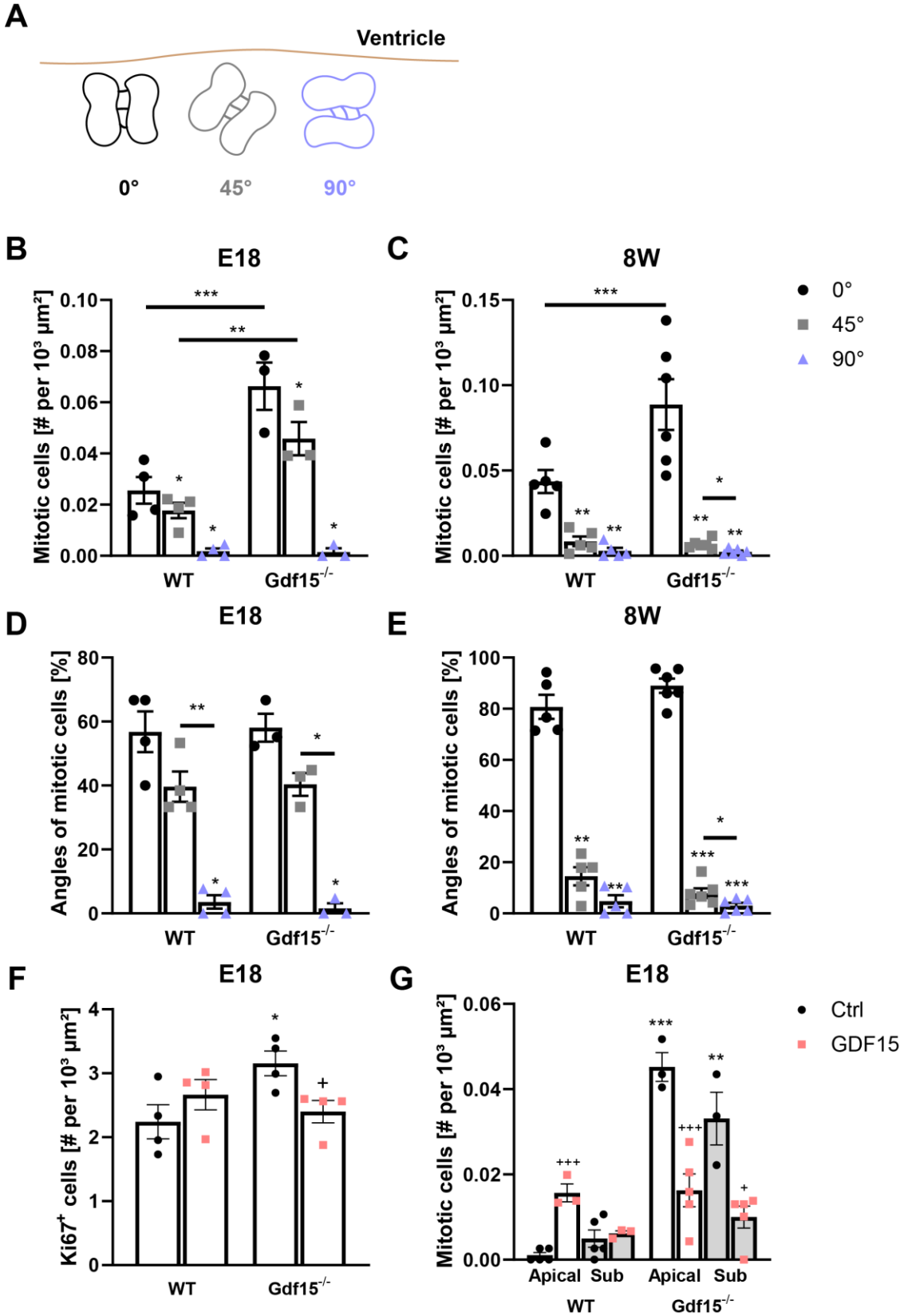

Figure 3: Mode of division is not changed by Gdf15 KO.
(A) Sketch illustrating the different division modes determined by the angle of the mitotic spindle relative to an orthogonal axis to the ventricular surface. Categories were determined as follows: 0° = 0°-30°; 45° = 30°-60°; 90° = 60°-90°.

(B, C) Quantification of total number of mitotic cells according to angle of mitosis at E18 (B) and in adult animals (C).
(D, E) Quantification of mitotic cells according to angle normalized to total mitotic cells at E18 (D) and in adult animals (E).
(F, G) Quantification of $Ki67^{+}$ cells (F) or mitotic cells (G) in E18 GE whole mounts either incubated without (Ctrl) or with GDF15 overnight.
Bars represent mean ± SEM; $*/^{+}$ indicate significance: $*/^{+}p<0.05$, $**p<0.01$, $***/^{+++}p<0.001$; * indicates significance to respective WT control, $^{+}$ indicates significance to respective untreated control.

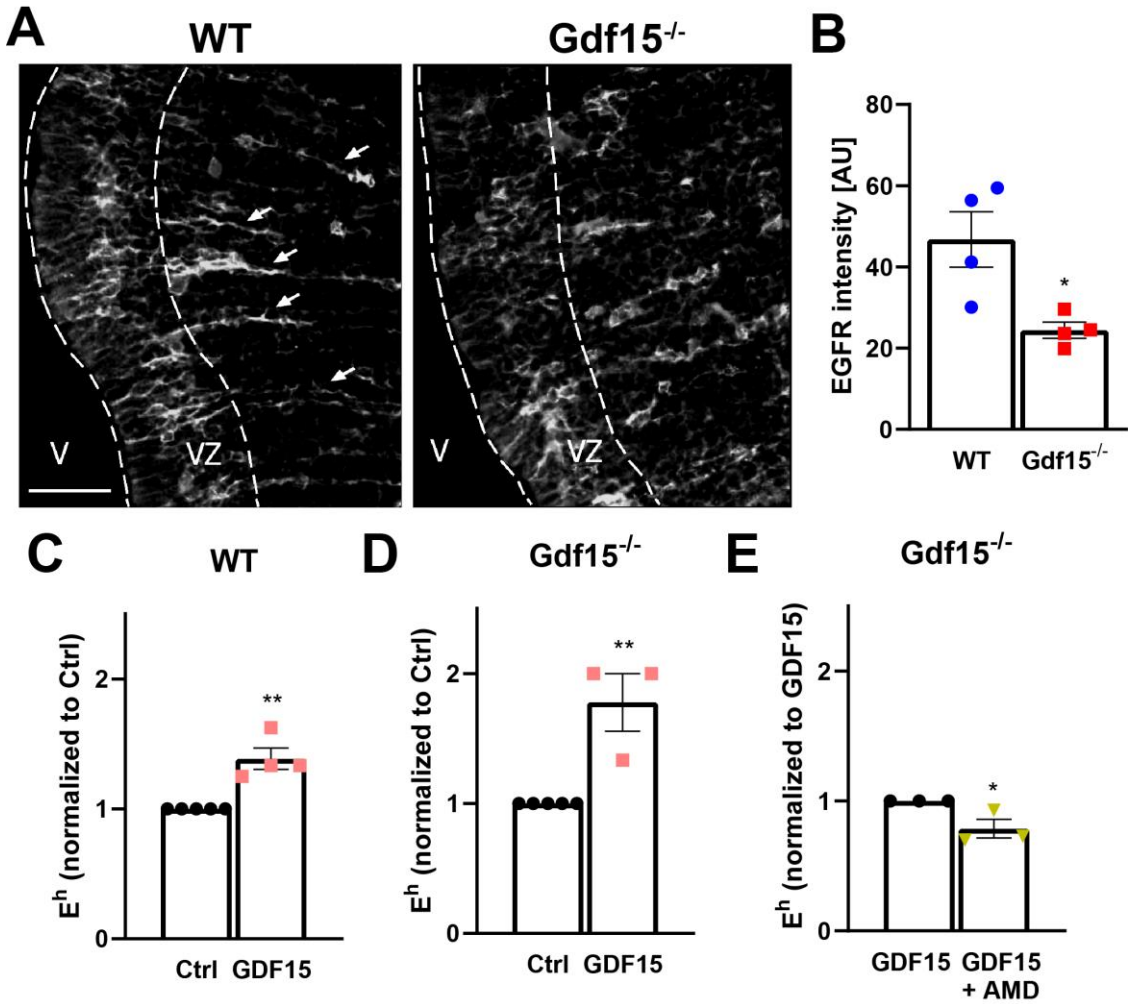

Figure 4: Lack of GDF15 reduces surface EGFR expression in the embryonic GE.
(A) Immunofluorescent staining for EGFR in slices from E18 mice. White arrows show the columns of radially oriented EGFR labelled cells that are absent in the Gdf15$^{-/-}$ GE. V = ventricle, VZ = ventricular zone; scale bar = 50 µm.
(B) Quantification of EGFR immunofluorescence intensity of the immunostaining shown in (A).
(C-E) Fold change in EGFR-expressing (E^{+}) cells isolated from the WT (C) and Gdf15$^{-/-}$ (D, E) GE at E18 as analysed by flow cytometry. Cells were either incubated in medium without or with GDF15, or with addition of CXCR4 antagonist AMD3100 (AMD), as indicated.
Bars represent mean ± SEM; * indicates significance: *$p<0.05$, **$p<0.01$.

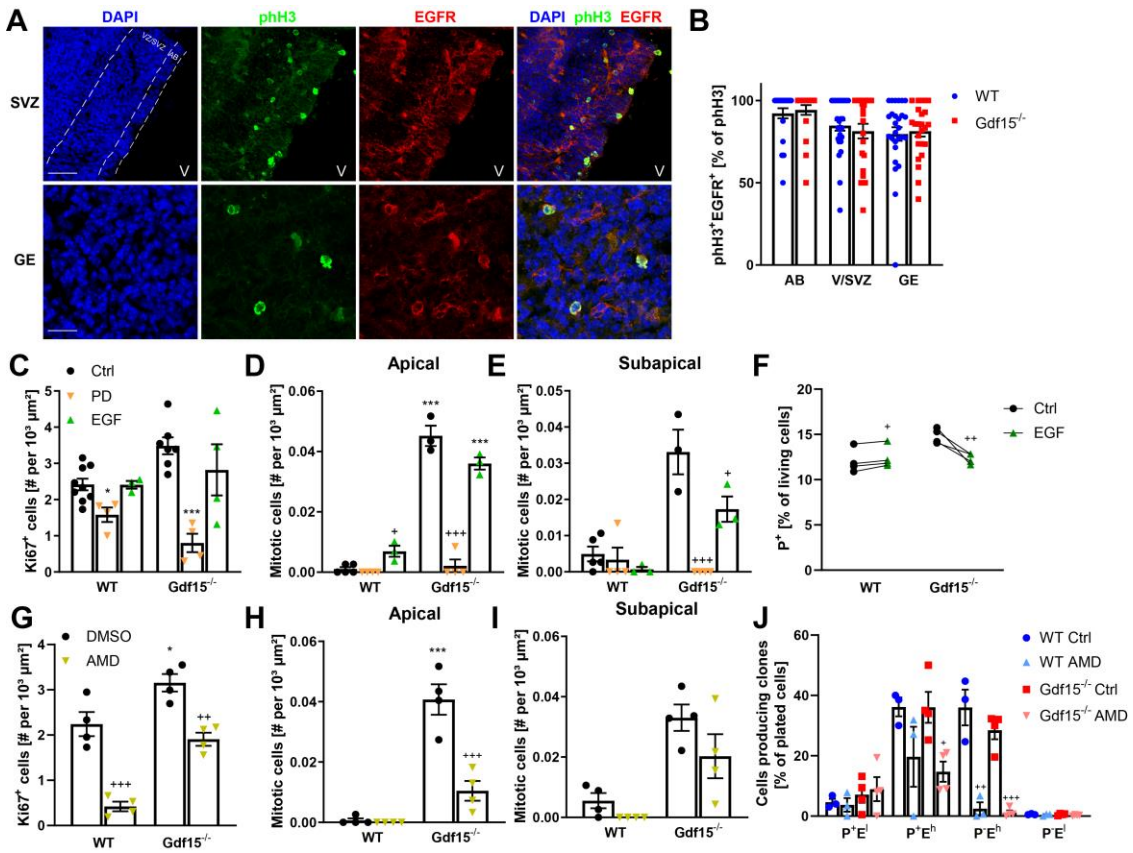

Figure 5: EGFR signalling is necessary for GE progenitor proliferation and is affected by lack of GDF15.

(A) Coronal sections of the GE germinal region of E18 WT and Gdf15$^{-/-}$ mice after immunostaining for phH3 (green) and EGFR (red). DAPI was used as nuclear counterstain. AB = apical border, VZ/SVZ = ventricular zone/subventricular zone, GE = deep ganglionic eminence, V = lateral ventricle. Scale bar = 37.5 µm.

(B) Quantification of phH3^{+} cells co-expressing EGFR in the different parts of the niche. AB = Apical border.

(C-E) Quantification of Ki67^{+} cells (C) or mitotic cells (D, E) at the apical side of E18 GE whole mounts either untreated (Ctrl) or incubated with EGFR-blocker PD158780 (PD) or exogenous EGF as indicated.

(F) Percentage of Prominin^{+} cells determined by FACS after overnight incubation with EGF. Data points represent individual animals, lines connect EGF-treated and untreated (Ctrl) data point of the for the same animal. Significance determined by paired t-test.

(G-I) Quantification of Ki67^{+} cells (G) or mitotic cells (H, I) at the apical side of E18 GE whole mounts either incubated with or with DMSO as control or CXCR4-blocker AMD3100 overnight.

(J) Clonal analysis of cells treated with AMD3100 after FACS sort.

Bars represent mean ± SEM; */$^{+}$ indicate significance: */$^{+}$p<0.05, **/$^{++}$p<0.01, ***/$^{+++}$p<0.001; * indicates significance to respective WT control, $^{+}$ indicates significance to respective untreated control.

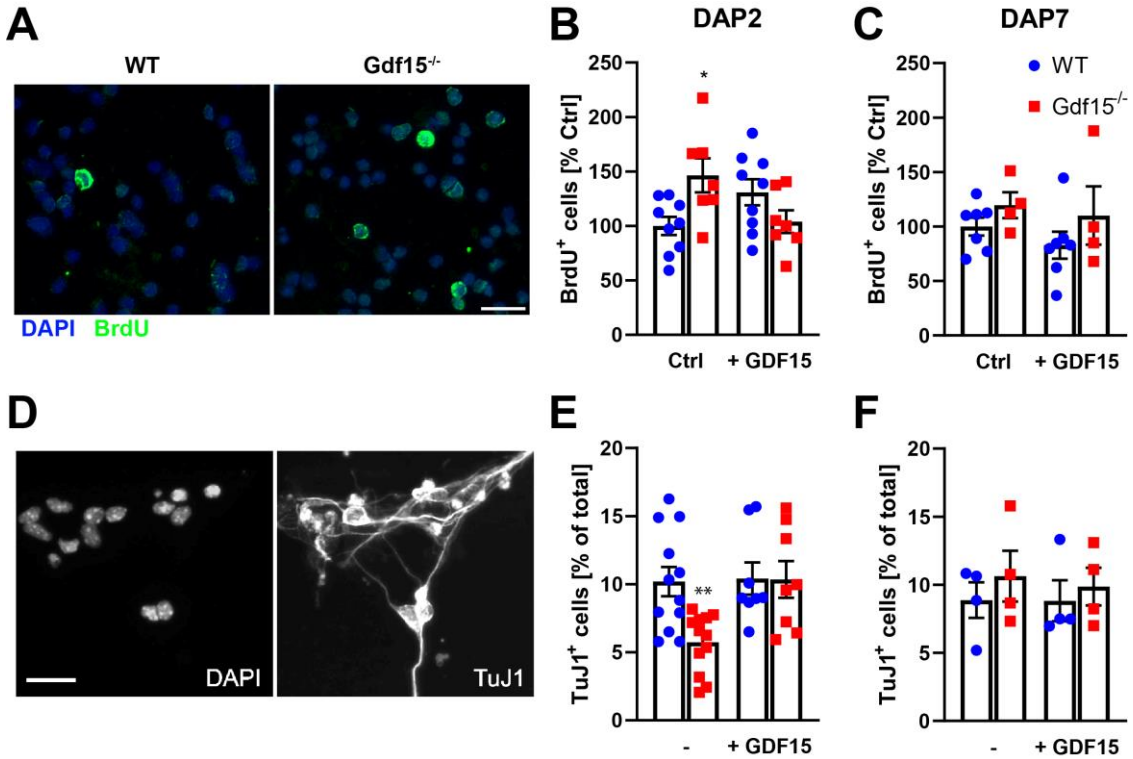

Figure 6: Primary Gdf15$^{-/-}$ cell cultures show a transient change in proliferation and neurogenesis.

(A) BrdU^{+} cells (green) and DAPI counterstaining of the nuclei (blue) in WT and Gdf15$^{-/-}$ control neurosphere cultures fixed two days after plating (DAP) in differentiation medium. BrdU was added to the culture medium 24h before fixation. Scale bar = 20 µm.

(B, C) Quantitative analysis of BrdU^{+} cells fixed two days (B) or seven days after induction of differentiation (C), with recombinant GDF15 added during differentiation (+GDF15) or without (Ctrl).

(D) Representative examples of neurosphere cultures derived from the E18 GE fixed seven days after the induction of differentiation and stained for TuJ1. DAPI was used for nuclear counterstain. Scale bar = 20 µm.

(E, F) Quantitative analyses of the number of TuJ1^{+} neurons in cultures fixed seven (E) and ten (F) days after the induction of differentiation and treated with exogenous GDF15 during the entire phase of differentiation (GDF15) or left untreated (Control) as indicated.

Bars represent mean ± SEM; * indicates significance: *$p<0.05$.

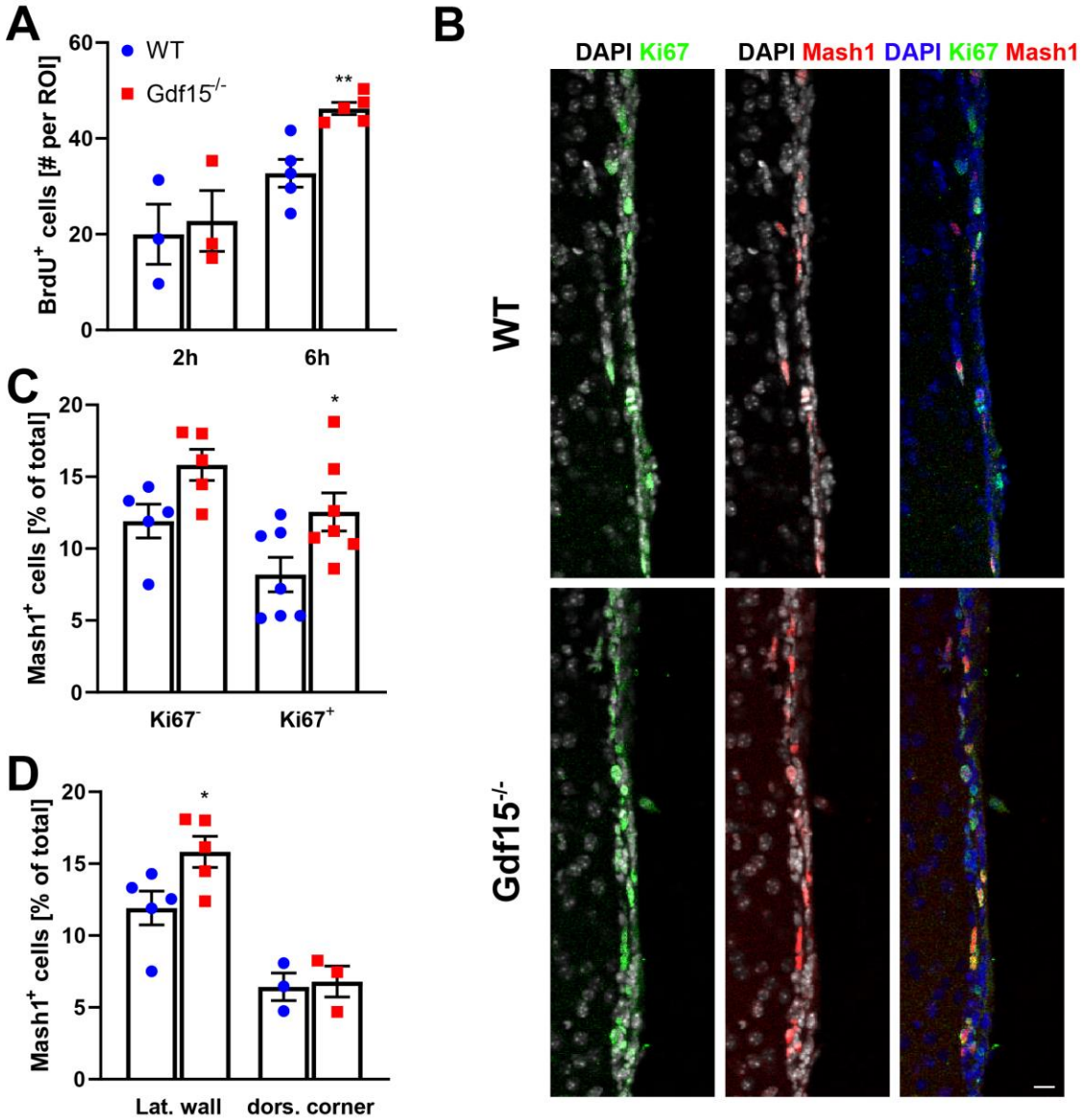

Figure 7: Increased proliferation in Gdf15$^{-/-}$ animals leads to an increase in Mash1^{+} progenitors in the lateral-ventral V/SVZ.

(A) Quantitative analysis of the percentage of DAPI stained nuclei displaying BrdU immunoreactivity per region of interest (ROI) within the GE of E18 GE from WT and Gdf15$^{-/-}$ embryos 2 and 6 hours after BrdU injection.

(B) Coronal sections of the V/SVZ of adult WT and Gdf15$^{-/-}$ mice after immunostaining for Ki67 (green) and Mash1 (red). DAPI was used as nuclear counterstain. Scale bar = 20 µm.

(C, D) Quantitative analysis of the percentage of DAPI stained nuclei in the V/SVZ of the adult WT and Gdf15$^{-/-}$ animals immunoreactive to MASH1 and displaying Ki67 immunoreactivity as indicated. Lat. wall = lateral wall, dors. corner = dorsolateral corner.

Bars represent mean ± SEM; * indicates significance: *$p<0.05$, **$p<0.01$.

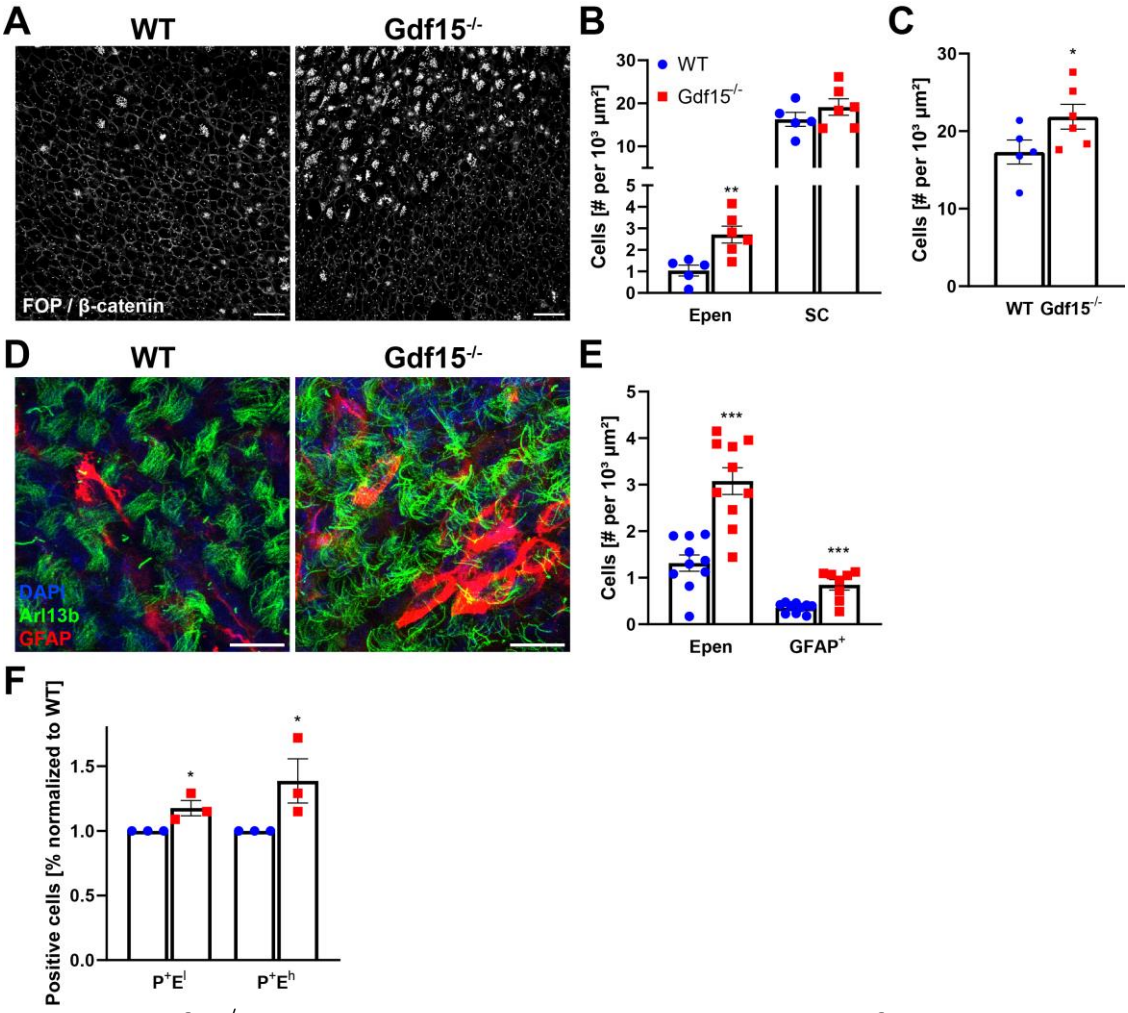

Figure 8: Gdf15$^{-/-}$ animals have persistently increased number of ependymal cells and GFAP^{+} apical NSCs.

(A) Whole mounts of the E18 lateral GE immunofluorescently labelled with basal body marker FOP, to label cilia, and β-catenin, to highlight cell-cell-contact. Scale bar = 20 µm.

(B, C) Quantification of cells in (A) that contain multiple basal bodies (ependymal cells, Epen) and single-ciliated cells (SC; B) as well as total cells (D).

(D) Whole mounts of the adult lateral V/SVZ immunofluorescently labelled with Arl13b, to label cilia, and GFAP, to label radial glia-like cells. Scale bar = 20 µm.

(E) Quantification of cells in (D) displaying multiple cilia (Epen) or displaying GFAP immunoreactivity (GFAP^{+}).

(F) FACS analysis of dissociated E18 GE cells labelled with antibodies against Prominin-1 (P), displayed according to high (E^{h}) or low levels of EGFR (E^{l}).

Bars represent mean ± SEM; * indicates significance: *$p<0.05$, **$p<0.01$.